A Novel Reaction Kinetics Model for Estimating the Carbon Content into Hydrothermal Carbonization Products

Michela Lucian, Giovanni Piro, Luca Fiori*

University of Trento, Dept. of Civil, Environmental and Mechanical Engineering, via Mesiano 77 - 38123 Trento, Italy
luca.fiori@unitn.it

This paper presents an original reaction kinetics model as a tool for estimating the carbon yield and distribution among the product phases originating from hydrothermal carbonization (HTC) of biomass. The kinetics model, developed in MATLAB^{TM}, was used in a best fitting routine with HTC experimental data obtained for a representative ligno-cellulosic biomass (grape marc) and it is easily applicable to any kinds of feedstock. Levenberg–Marquardt algorithm was used for best fitting. The HTC reaction pathway was described through a lumped model, in which biomass is converted into solid (primary and secondary char), liquid and gaseous products. Runge-Kutta method was used to solve the system of 6 differential equations - mass balances - accounting for the different HTC lumped reactions, through the estimation of 5 Arrhenius kinetics parameters (k_1 k_2 k_3 k_4 k_5). The k_i parameters were used to graphically determine the pre-exponential factors ($k_{0,i}$) and the activation energy ($E_{a,i}$) values for each reaction. Modelling predictions are in very good agreement with experimental data, i.e. carbon content calculated from hydrochar and gas mass yields and ultimate analysis data. For all the examined conditions (T=180-250 °C, t=0-8 h), the model fitting errors resulted lower than 10%. The developed reaction kinetics model is therefore a reliable tool for the prediction of carbon distribution among HTC products.

1. Introduction

The continuous growth of world population has heightened the need to find a way for valorizing agricultural and agro-industrial wastes. Among the many potential technologies to treat such residues, one of the most promising is HydroThermal Carbonization (HTC). This process allows organic waste to be upgraded into a carbon-rich material called hydrochar. Hydrochar finds application as fertilizer, fuel (Castello et al. 2014) or advanced carbon material (Purnomo et al. 2018). HTC is a thermo-chemical process that occurs in subcritical water under autogenous pressure at low temperatures (160-300 °C) and residence times typically up to 8 h. This technology has attracted the attention of researchers and companies (Carborem 2017) for its high energy efficiency and feasibility (Lucian & Fiori 2017).
HTC produces a solid fuel with higher energy density (Volpe et al. 2018) and hydrophobicity than the original material.
In recent years, many research groups have focused on how HTC process parameters influence the chemical and physical characteristics of hydrochar. Despite the large amount of studies available in literature regarding HTC, the kinetics of this process is still lacking of a deep investigation. Few years ago, our research group (Baratieri et al. 2015) suggested a simple kinetics model for HTC based on a two-step reaction mechanism. In that model, the original biomass (A) forms an intermediate product (B) that partially degrades to form the final product C (the hydrochar). In the meanwhile, two reactions in parallel to those giving compounds B and C take place, leading to the formation of gaseous products (V1 and V2). The model lacked in considering the organics present in the HTC liquid phase. The model was calibrated using hydrochar yield experimental data (Baratieri et al. 2015).
By using a different approach, this paper presents an innovative HTC reaction kinetics model capable to predict the carbon distribution into all HTC products: hydrochar, liquid and gas phases. The Arrhenius kinetics parameters (pre-exponential factor and activation energy) of the involved reactions were obtained for grape marc (GM) - as a reference case study - at different HTC conditions.

2. Materials and Methods

The kinetics model, developed using MATLAB[TM] software, was tested on HTC experimental data obtained for GM samples, and reported in our previous study (Basso et al. 2016). The HTC tests were performed in duplicate at 180, 220, and 250 °C, at residence times of 1, 3, and 8 h, keeping fixed the solid load (dry biomass to water ratio equal to 0.19). Fiori et al. (2014) described in detail the HTC system used for such experiments.

Figure 1 shows the lumped scheme used in the kinetics model which describes in a simplified way the complex reaction pathways occurring during HTC.
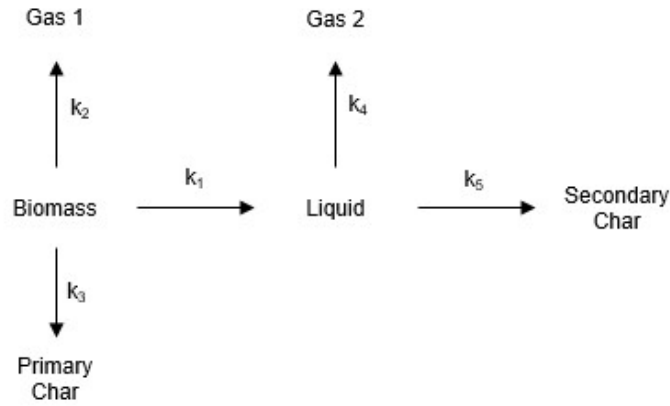

Figure 1: The lumped model used to describe HTC reaction paths

In details, the first reaction step (Reaction 1, Biomass→Liquid) represents the hydrolysis and dissolution processes through which the biomass components are partially degraded into oligomers and monomers deriving from hemicellulose and cellulose (Funke et al. 2010). These liquid products can undergo further reactions and form stable liquid compounds or highly reactive intermediates - especially 5-HMF (Funke et al. 2010, Libra et al. 2011). These reactive intermediates can back polymerize producing a solid residue named "coke" or "secondary char" (Reaction 5, Liquid→Secondary char) (Volpe & Fiori 2017). In parallel, a solid-to-solid reaction (Reaction 3, Biomass→Primary char) occurs via dehydration of the initial biomass. Thus, a certain amount of water is removed from the biomass, leading to a significant reduction of the H/C and O/C ratios in the produced hydrochar. When dehydration has terminated, decarboxylation and decarbonylation reactions occur (Funke et al. 2010). These reactions lead to the elimination of CO_2 and CO directly from the biomass (Reaction 2, Biomass→Gas 1). In addition, liquid compounds resulting from hydrolysis could decompose into small gaseous molecules, mainly CO_2 (Reaction 4, Liquid→Gas 2), or back-polymerize and condense as a solid phase (Reaction 5, Liquid→Secondary char), as previously mentioned. The kinetics parameters k_i (k_1 k_2 k_3 k_4 k_5) in Figure 1 are the kinetics constants of the five reactions i and are defined within the model through the Arrhenius equation Eq(1):

$$k_i = k_{0,i} e^{-\frac{E_{a,i}}{RT}} \qquad\qquad i = 1,.....5; \tag{1}$$

The kinetics model is thus represented by a system of non-linear differential equations - Eq(2) - in which C_B, C_L, C_{G1}, C_{HC1}, C_{G2} and C_{HC2} are the molar concentrations (mol/L) of carbon in biomass (B), liquid phase (L), gas 1 (G1), primary char (HC1), gas 2 (G2) and secondary char (HC2), respectively, and t is reaction time.

$$\frac{\partial C_B}{\partial t} = -k_1 C_B - k_2 C_B - k_3 C_B \tag{2}$$

$$\frac{\partial C_L}{\partial t} = k_1 C_B - k_4 C_L - k_5 C_L^n$$

$$\frac{\partial C_{G1}}{\partial t} = k_2 C_B$$

$$\frac{\partial C_{HC1}}{\partial t} = k_3 C_B$$

$$\frac{\partial C_{G2}}{\partial t} = k_4 C_L$$

$$\frac{\partial C_{HC2}}{\partial t} = k_5 C_L^n$$

The carbon molar concentration in component X (B, L, G1, HC1, G2, HC2), C_X, is expressed as:

$$C_X = \frac{n_{c,X}}{(V_B + V_W)} \tag{3}$$

Where $n_{c,X}$ is the number of moles of carbon in component X and term $V_B + V_W$ represents the sum of the volumes (expressed in L) of biomass as received and distilled water added to the HTC reactor to get the set solid load. The system of differential equations was solved numerically using Runge-Kutta method, by means of a routine that estimates the k_i parameters through an error minimization method called Levenberg-Marquardt method. This "curve-fitting" tool is used commonly and extensively in computing for non-linear least squares problems (Almagrbi et al. 2014, Urych 2014).

The error function $F(k_i, n)$ - n being the reaction order of reaction 5 - is represented by Eq(4) and has as input variables experimental data (apex: "exp") obtained at different HTC reaction times and the corresponding data computed by the model (apex: "mod"). The subscript j refers to the various reaction times at which experimental data are available.

$F(k_i, n)$ was thus minimized in order to get the kinetics parameters k_i and n.

$$F(k_i, n) = \sum_j |C_{S,j}^{exp} - C_{S,j}^{mod}| + \sum_j |C_{L,j}^{exp} - C_{L,j}^{mod}| + \sum_j |C_{G,j}^{exp} - C_{G,j}^{mod}| \tag{4}$$

$$C_{S,j}^{exp} = \frac{n_{c,HC}}{(V_B + V_W)} = \frac{m_{c,HC}}{M_c} \cdot \frac{1}{(V_B + V_W)} = \frac{m_{HC}\%c_{HC}}{M_c} \cdot \frac{1}{(V_B + V_W)} = \frac{Y_{HC}m_{B,0}\%c_{HC}}{M_c} \cdot \frac{1}{(V_B + V_W)} \tag{5}$$

$$C_{S,j}^{mod} = C_{B,j}^{mod} + C_{HC1,j}^{mod} + C_{HC2,j}^{mod} \tag{6}$$

$$C_{L,j}^{exp} = C_{B,0}^{exp} - C_{S,j}^{exp} - C_{G,j}^{exp} \tag{7}$$

$$C_{G,j}^{exp} = \frac{n_{c,G}}{(V_B + V_W)} = \frac{n_{CO_2}}{(V_B + V_W)} = \frac{P\,V_{CO_2}}{R\,T} \cdot \frac{1}{(V_B + V_W)} \tag{8}$$

$$C_{G,j}^{mod} = C_{G1,j}^{mod} + C_{G2,j}^{mod} \tag{9}$$

Letters S, L, and G are used to identify solid, liquid, and gas phases. Letters m, M, and Y indicate respectively mass (g), molar mass (g/mol), and solid mass yield (*i.e.* hydrochar yield: $m_{HC}/m_{B,0}$, dry basis). Subscripts c, HC and 0 refer respectively to carbon, hydrochar, and initial value. % indicates the percentage on a dry mass basis. The solid, after the HTC reaction started, consists of hydrochar: Eq(5). Conversely, in the model (Eq(6)) the solid consists of the biomass - whose amount decreases during HTC while its composition is considered constant: Eq(2) - plus primary char HC1 and secondary char HC2. In Eq(8), P and T are the atmospheric pressure (1 atm) and the room temperature (293.15 K), respectively; V_{CO2} is the volume of the gas experimentally measured, which was assumed to consist of CO_2 only; R is the gas constant (0.08206 L atm/K mol). In the model (Eq(9)), the gas consists of the sum of G1 and G2. The experimental values for the liquid were calculated by difference (Eq(7)), while the relevant model values were obtained by solving Eq(2).

The available experimental data were the input values V_B, V_W, and $m_{B,0}$ and the HTC output values Y_{HC}, $\%c_{HC}$ (from hydrochar elemental analysis), and V_{CO_2}.

Based on the experimental data available for the HTC of grape marc, $F(k_i, n)$ was minimized for three reaction times (1, 3 and 8 h) at each of three HTC temperatures (180, 220 and 250 °C). It is worth mentioning that considering in Eq(4) the term related to the liquid phase (which could be actually omitted without compromising the correctness of the equation) allowed the software to converge faster towards the solution of the minimization problem.

Once the k_i parameters were estimated, the Arrhenius plot ($\ln k_i$ vs 1/T) was used as a graphical method to determine the activation energy $E_{a,i}$ and the pre-exponential factor $k_{0,i}$ of the lumped HTC reactions considered.

3. Results and discussion

Table 1 reports the value of the kinetics parameters k_i estimated by the model.

Table 1: Kinetics constants (k_i) and reaction order (n) for the lumped reactions in Figure 1

Kinetics parameters	180 °C	220 °C	250 °C
k_1 (s^{-1})	0.1126	0.1243	0.2015
k_2 (s^{-1})	0.0094	0.0204	0.0372
k_3 (s^{-1})	0.3886	0.3894	0.5216
k_5 (s^{-1})	0.1160	0.1172	0.1187
n (-)	1.0006	1.0008	1.0297

The kinetics parameters k_i increase with temperature, as expected. In addition, Table 1 shows that k_3 is the highest in value at all the HTC temperatures and this suggests that conversion of biomass into primary char is the most favored reaction path. The Biomass→Liquid conversion (k_1) is also quite fast, while the reactions producing gases are the slowest: for all the temperatures, k_4 was even equal to zero and therefore it has not been reported in Table 1. The reaction order n of secondary char formation path is slightly higher than 1 in all the cases, and increases with temperature. The production of secondary char (k_5) is not negligible.

The results regarding carbon distribution among the various HTC components are reported in Figure 2 a, c, e. In Figure 2, the vertical dotted lines represent the time when the HTC reactor reached the set temperature, and from which the experimental reaction time has started to be counted. Our simulations, based on the system of differential equations represented by Eq(2), conversely considered time zero when the HTC reactor started to be heated to reach the set temperature (16, 22, and 28 min to reach 180, 220 and 250 °C, respectively).

Carbon distribution is expressed here in terms of carbon recovery CR, defined in Eq(10) as the ratio of the number of moles of carbon in component X ($n_{c,X}$) to the number of moles of carbon in the raw biomass ($n_{c,B,0}$), both on a dry basis (Hwang et al. 2012):

$$CR_X = \frac{n_{c,X}}{n_{c,B,0}} \tag{10}$$

CR allows understanding easily the distribution of carbon among the different HTC phases. In contrast to alcoholic fermentation, in which two out of six carbon atoms are released as CO_2, or anaerobic digestion, in which about half of the carbon is released as CO_2, during HTC the largest part of the initial carbon is recovered into the hydrochar and only small fractions are transferred to the gas and liquid phases. Thus, the parameter "carbon recovery" is highly representative and is used here as a key-variable for outlining the carbon distribution among the various HTC phases.

Figure 2 b, d, f shows the model predictions together with the experimental values of CR for both solid (hydrochar) and gas phases. The carbon recovery in the gas phase increases progressively with time at all the HTC temperatures; the higher the temperature, the higher CR. The carbon recovery in the solid phase decreases during reaction up to about 3 h for all the three temperatures, and then tends to stabilize.

The model fits perfectly the experimental data at 180 °C and very well the data at 220 °C and 250 °C. As a whole, the model performs satisfactorily: the differences between model predictions and experimental data, calculated by means of Eq(4), result lower than 10% in all the cases.

The Arrhenius plots for the different kinetics constants k_i are shown in Figure 3. The activation energies $E_{a,i}$ and the pre-exponential factors $k_{0,i}$ for each HTC reaction path have been determined from the slopes of the curves ($-E_{a,i}/R$) and the intercepts with the y-axis: Figure 3. The values of the Arrhenius parameters are reported in Table 2. $E_{a,2}$ (Biomass→Gas 1) assumes the highest values. $E_{a,1}$, which refers to Biomass→Liquid path, is also quite high. The activation energies relevant to the formation of primary and secondary char ($E_{a,3}$ and $E_{a,5}$, respectively) are conversely relatively small, thus supporting what previously reported on the relative rate of the various HTC reaction paths. However, it is worth noticing that the pre-exponential factors follows exactly the same trend as the activation energies: the higher $E_{a,i}$, the higher $k_{0,i}$. Thus, the data of Table 2 are likely affected by the interrelation between $E_{a,i}$ and $\ln k_{0,i}$, which can be expressed through a linear relationship (Liu et al. 2003):

$$\ln k_{0,i} = a\, E_{a,i} + b \tag{11}$$

Eq(11) highlights that a change in value of activation energy leads to a change in value of pre-exponential factor, and vice-versa. This means that a reduction in reaction rate expected from an increase in $E_{a,i}$ does not occur in the case this is compensated by an opportune increase in $k_{0,i}$ (Fiori et al. 2012). Given this, the data of Table 1 allow for a straighter at a glance comparison among the relative rates of the reactions involved in the kinetics scheme modeled.
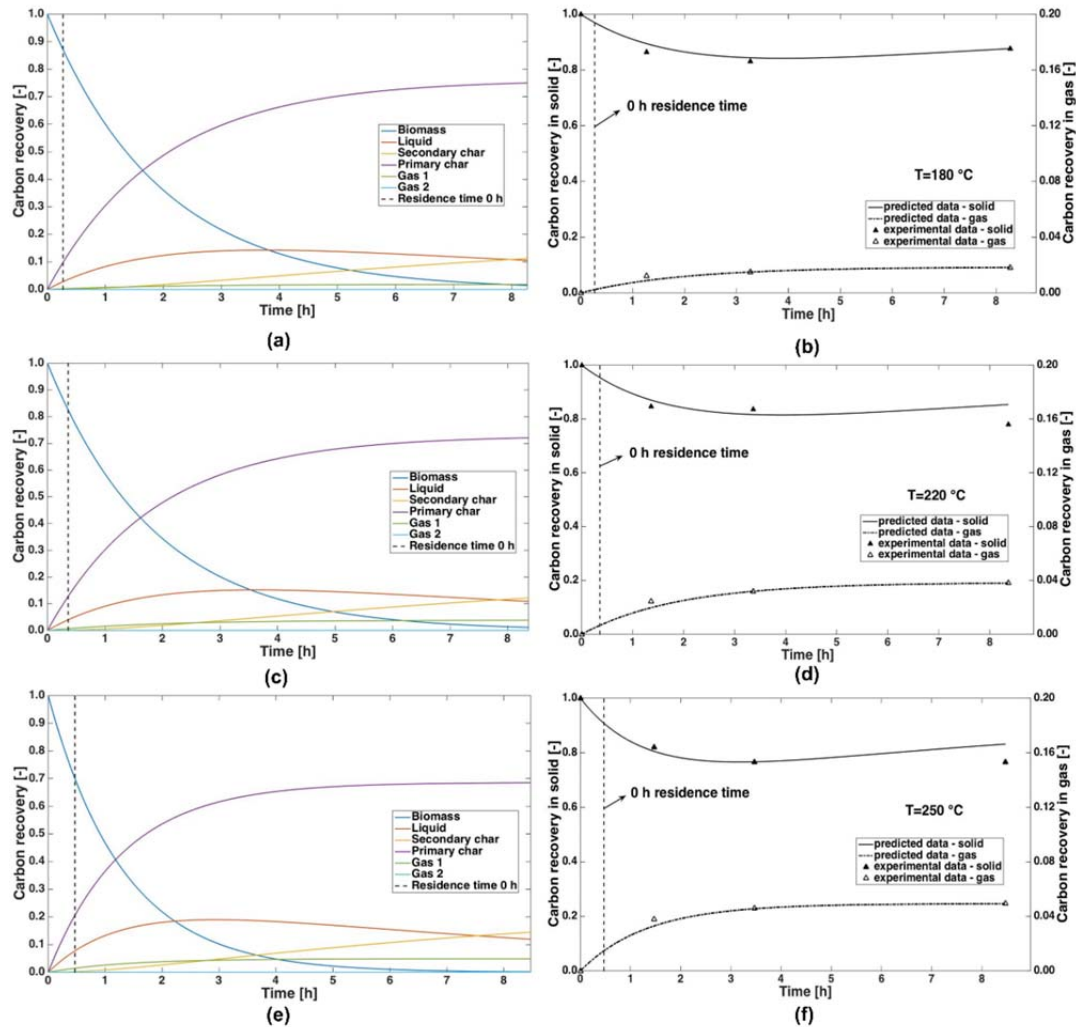

Figure 2: Carbon recovery vs time into HTC product phases (B, L, HC1, HC2, G1, G2) at a) 180 °C, c) 220 °C, e) 250 °C, and in solid and gas phases at b) 180 °C, d) 220 °C, f) 250 °C
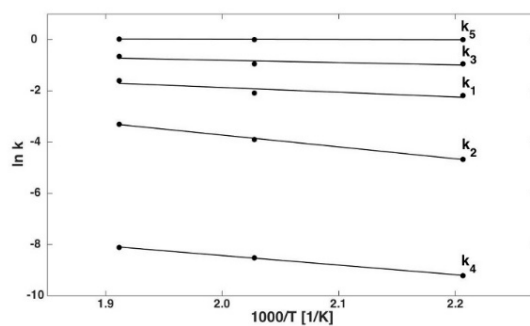

Figure 3: Arrhenius plot for the determination of activation energies ($E_{a,i}$) and pre-exponential factors ($k_{0,i}$)

Table 2: Arrhenius parameters obtained by the kinetics model

Arrhenius parameters	
$k_{0,1}$ (s^{-1})	6.2638
$k_{0,2}$ (s^{-1})	251.720
$k_{0,3}$ (s^{-1})	2.7885
$k_{0,5}$ (s^{-1})	1.2122
$E_{a,1}$ (kJ/mol)	15.3813
$E_{a,2}$ (kJ/mol)	38.4465
$E_{a,3}$ (kJ/mol)	7.5934
$E_{a,5}$ (kJ/mol)	0.7391

4. Conclusions

This paper proposes a novel reaction kinetics model to estimate the carbon recovery and its distribution among the HTC product phases. Modelling predictions are in very good agreement with experimental data, *i.e.* with carbon content calculated from hydrochar and gas mass yields and hydrochar ultimate analysis data. For all the examined conditions (T=180-250 °C, t=0-8 h), the model fitting errors resulted lower than 10%. The developed reaction kinetics model is therefore a reliable tool for the prediction of carbon distribution among HTC products, and the next step in the research will be testing the model with a much wider set of experimental data relevant to many different substrates.

Reference

Almagrbi, A.M. et al., 2014. Determination of kinetic parameters for complex transesterification reaction by standard optimisation methods. Hemijska Industrija, pp.149–159.

Baratieri, M. et al., 2015. Kinetic and Thermal Modeling of Hydrothermal Carbonization Applied to Grape Marc. Chemical Engineering Transactions, 43, pp.505–510.

Basso, D. et al., 2016. Agro-industrial waste to solid biofuel through hydrothermal carbonization. Waste Management, 47, pp.114–121.

Castello, D., Kruse, A. & Fiori, L., 2014. Supercritical water gasification of hydrochar. Chemical Engineering Research and Design, 92, pp.1864-1875.

Carborem S.r.l., 2017, Homepage. <www.carborem.com> accessed 21.12.2017.

Fiori, L. et al., 2014. Hydrothermal carbonization of biomass: Design of a batch reactor and preliminary experimental results. Chemical Engineering Transactions, 37, pp.55–60.

Fiori, L. et al., 2012. Modeling of the devolatilization kinetics during pyrolysis of grape residues. Bioresource Technology, 103(1), pp.389–397.

Funke, A., Ziegler, F. & Berlin, T.U., 2010. Hydrothermal carbonization of biomass: A summary and discussion of chemical mechanisms for process engineering. Biofuels, Bioproducts and Biorefining, 4, pp.160–177.

Hwang, I. et al., 2012. Recovery of solid fuel from municipal solid waste by hydrothermal treatment using subcritical water. Waste Management, 32(3), pp.410–416.

Libra, J.A. et al., 2011. Hydrothermal carbonization of biomass residuals: a comparative review of the chemistry, processes and applications of wet and dry pyrolysis. Biofuels, 2(1), pp.71–106.

Liu, N., Wang, B. & Fan, W., 2003. Kinetic Compensation Effect in the Thermal Decomposition of Biomass in Air Atmosphere. In Fire Safety Science-Proceedings of the seventh international symposium. pp. 581–592.

Lucian, M. & Fiori, L., 2017. Hydrothermal Carbonization of Waste Biomass: Process Design, Modeling, Energy Efficiency and Cost Analysis. Energies, 10, p.211.

Purnomo, C.W., Castello, D. & Fiori, L., 2018. Granular activated carbon from grape seeds hydrothermal char. Applied Sciences, 8, p.331.

Urych, B., 2014. Determination of kinetic parameters of coal pyrolysis to simulate the process of Underground Coal Gasification (UCG). Journal of Sustainable Mining, 13(1), pp.3–9.

Volpe, M. & Fiori, L., 2017. From olive waste to solid biofuel through hydrothermal carbonisation: The role of temperature and solid load on secondary char formation and hydrochar energy properties. Journal of Analytical and Applied Pyrolysis, 124, pp.63–72.

Volpe, M., Goldfarb J.L. & Fiori, L., 2018. Hydrothermal carbonization of Opuntia ficus-indica cladodes: Role of process parameters on hydrochar properties. Bioresource Technology, 247, pp.310–318.